View metadata, citation and similar papers at core.ac.uk
brought to you by CORE
provided by National Chung Hsing University Institutional Repository

China Ocean Eng., Vol. 26, No. 1, pp. 167 – 176
© 2012 Chinese Ocean Engineering Society and Springer-Verlag Berlin Heidelberg
DOI 10.1007/s13344-012-0012-6, ISSN 0890-5487

Wave Height Transformation and Set-up Between A Submerged Permeable Breakwater and A Seawall*

TSAI Ching-piao (蔡清标)[a, 1], YU Chien-hung (余建弘)[a],
CHEN Hong-bin (陈鸿彬)[b] and CHEN Hsin-yu (陈信佑)[a]

[a] *Department of Civil Engineering, National Chung Hsing University*, *Taichung 402, China*
[b] *Department of Sports, Health, and Leisure, Chihlee Institute of Technology*, *Taipei 220, China*

(Received 13 April 2010; received revised form 5 May 2011; accepted 28 July 2011)

ABSTRACT

In this study, we investigated wave transformation and wave set-up between a submerged permeable breakwater and a seawall. Modified time-dependent mild-slope equations, which involve parameters of the porous medium, were used to calculate the wave height transformation and the mean water level change around a submerged breakwater. The numerical solution is verified with experimental data. The simulated results show that modulations of the wave profile and wave set-up are clearly observed between the submerged breakwater and the seawall. In contrast to cases without a seawall, the node or pseudo-node of wave height evolution can be found between the submerged breakwater and the seawall. Higher wave set-up occurs if the nodal or pseudo-nodal point appears near the submerged breakwater. We also examined the influence of the porosity and friction factor of the submerged permeable breakwater on wave transformation and set-up.

Key words: *wave height transformation*; *water piling-up*; *wave set-up*; *submerged permeable breakwater*; *seawall*; *time-dependent mild-slope equations*

1. Introduction

Taiwan experiences 3.5 typhoons per year on average. As a result, coastal disasters, including beach erosion and coastal inundation, often occur in many low-lying coastal areas during the storms. Since 1973, traditional seawalls have been built along many coastlines of Taiwan to help mitigate these hazards. The total length of seawalls now is about 542 km, which is nearly half of the total coastline of Taiwan Island. However, as a result of the failure of the seawall structure or serious toe scours, some seawalls have not completely prevented the occurrence of coastal disasters. In response, multiple countermeasures, such as a submerged breakwater constructed in front of a seawall, have been proposed to create a new system of shoreline protection.

Numerous theoretical and numerical investigations have been completed to explore wave transformation over submerged or low-crested breakwaters, such as Rojanakamthorn *et al*. (1989), Losada *et al*. (1996), Liu *et al*. (1999), Hur and Mizutani (2003) and Tsai *et al*. (2006). Many laboratory and field investigations have also been performed, such as Diskin *et al*. (1970), Dattatri *et al*. (1978), Davies and Kriebel (1992), Loveless *et al*. (1998) and Garcia *et al*. (2004). It is well known

* The work was financially supported by The Science Council of Taiwan under Grant No. 95-2221-E-005-154.
1 Corresponding author. E-mail: cptsai@dragon.nchu.edu.tw

that an incident wave may decay over a permeable submerged breakwater as a result of energy dissipation, but the mean water level set-up may also be observed behind a breakwater, arising from the wave breaking and the water piling-up (Diskin *et al*., 1970; Méndez *et al*., 2001; Garcia *et al*., 2004).

Regardless of whether a submerged or low-crested breakwater was permeable or impermeable, the submerged structure has been investigated without consideration of the existence of a seawall behind it. However, in the case of a combined submerged breakwater and seawall, wave transformation over the submerged structure will become more complex because of the interaction between transmitted waves and waves reflected from the seawall. In addition, the phenomenon of water level set-up behind a submerged breakwater, arising from waves breaking and water piling-up, will also be influenced by the existence of the seawall, which has not been sufficiently considered in previous studies.

In the present study, we report the numerical results of wave height variations and water level variations between a submerged permeable breakwater and a seawall. The formulations of the time-dependent mild-slope equations are outlined first, and then the numerical results are presented. The influences of the types of seawall, the porosity and friction factor of the submerged permeable breakwater, and the incident wave conditions on the wave transformation are then discussed.

2. Formulations

The boundary value problem considered in this study is for wave transformation between a permeable submerged breakwater and a seawall, which can be formulated based on the wave transformation over a bottom with porous medium, as shown in Fig. 1. Referring to Chen *et al*. (2006), the time-dependent mild-slope equations involving the parameters of the porous medium can be given as:

$$\frac{\partial \eta}{\partial t}+\frac{1}{n}\frac{\partial (nQ)}{\partial x}=0; \tag{1}$$

$$\frac{\partial Q}{\partial t}+c^2\frac{\partial \eta}{\partial x}=0, \tag{2}$$

where η is the surface elevation; $Q = c\eta$ is the flow rate of linear progressive waves; c is defined by ω/k, $\omega = 2\pi/T$, T being the wave period; and k is the wave number that can be determined from the relationship:

$$\omega^2 = gk\frac{\varepsilon_b[SH]\cosh kh+\alpha_b[CH]\sinh kh}{\varepsilon_b[SH]\sinh kh+\alpha_b[CH]\cosh kh}; \tag{3}$$

$$[SH]=\varepsilon_b\sinh kh_b\cosh kh+\alpha_b\cosh kh_b\sinh kh; \tag{4}$$

$$[CH]=\varepsilon_b\sinh kh_b\sinh kh+\alpha_b\cosh kh_b\cosh kh, \tag{5}$$

and n in Eq. (1) is given as:

$$n=\frac{1}{2}\left\{1+\frac{kh_b(\varepsilon_b\alpha_b)+kh\left[-\varepsilon_b^2(\sinh kh_b)^2+\alpha_b^2(\cosh kh_b)^2\right]}{[SH]\cdot[CH]}\right\}. \tag{6}$$

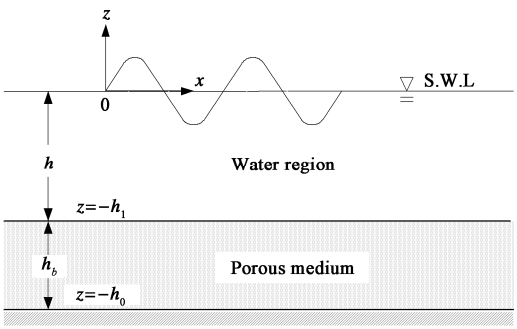

Fig. 1. Definitional sketch of waves propagating on a porous medium.

In the above equations, h is the water depth, h_b is the thickness of the porous medium, ε_b is the porosity of the medium, and $\alpha_b = C_r - if_b$. The coefficient f_b is the linearized friction factor. C_r is an inertial coefficient of flow in a porous medium and is defined as $C_r = 1 + C_M(1-\varepsilon_b)/\varepsilon_b$ (Sollitt and Cross, 1972), where C_M is the added mass coefficient. In the wave dispersion relationship, Eq. (3), the wave number is a complex variable, which can be solved by using the Newton-Raphson iteration scheme. The first mode of a complex solution can be obtained and expressed as $k = k_r + ik_i$, in which the imaginary part of wave number (k_i) represents the wave damping factor, while the real part (k_r) is the wave number defined as $k_r = 2\pi/L_p$, L_p being the wavelength.

By taking into consideration that wave breaking may occur over the submerged breakwater, a nonlinear wave shoaling corrector and the energy dissipation factor proposed by Tsai *et al*. (2001) are incorporated into the mild-slope equation. Eq. (2) is then modified as:

$$\frac{\partial Q}{\partial t} + c^2 \frac{\partial \eta}{\partial x} + fQ = 0, \tag{7}$$

in which $f = \delta f_e + (1-\delta) f_d$, f_e is the nonlinear wave shoaling correction factor, and f_d is the wave energy dissipation factor. δ is assumed to be one before wave breaking and zero after wave breaking. We used the energy dissipation factor, f_d, expressed by Watanabe and Dibajnia (1988) and given as:

$$\left.\begin{aligned} f_d &= \alpha_D \tan\beta \sqrt{\frac{g}{h}\frac{Q_m - Q_r}{Q_s - Q_r}} \\ Q_r &= \gamma_r ch, \quad Q_s = \gamma_s ch \end{aligned}\right\}, \tag{8}$$

in which $\tan\beta$ is the average bottom slope around the breaking point; the coefficients are set to $\alpha_D = 2.5$, $\gamma_s = 0.4(0.57 + 5.3\tan\beta)$ and $\gamma_r = 0.4(a/h)_b$; $(a/h)_b$ is the ratio of the wave amplitude to the water depth at the breaking point; Q_m is the amplitude of the actual flow rate of wave; Q_r is the amplitude of the flow rate of recovery waves; and Q_s denotes the amplitude of the wave-induced flow rate inside the surf zone of a beach with uniform slope. The energy dissipation factor, f_d, is set equal to zero outside the surf zone and in any region in which $Q_m < Q_r$.

The nonlinear wave shoaling corrector, f_e, expressed by Tsai *et al*. (2001) is given as:

$$f_e = \alpha_S \tan\beta \frac{c}{h} \tag{9}$$

in which

$$\alpha_S = \begin{cases} 0 & \text{for } Ur \le 30 \\ -\dfrac{4}{7} + m_1 + m_2 & \text{for } 30 \le Ur \le 50 \\ (3\sqrt{Ur} - 10\sqrt{3}) / (1.5\sqrt{Ur} - 2\sqrt{3}) + m_1 + m_2 & \text{for } 50 \le Ur \text{ to breaking point} \end{cases}; \tag{10}$$

and

$$m_1 = \frac{2n-1}{2n},\ m_2 = \frac{k_o h - h^2(k^2 + k_o^{\ 2})}{4n^2 \sinh^2 kh}, \tag{11}$$

where k_o is the wave number at deep water. In Eq. (10), $Ur = gHT^2 / h^2$ is the local Ursell parameter defined by Shuto (1974), and H is the local wave height.

We used the wave breaking criteria on a submerged permeable breakwater proposed by Rojanakamthorn *et al*. (1990), which is given by

$$\frac{H_b}{L_o} = 0.127 \tanh \frac{2\pi (h_0)_b}{L_o}, \tag{12}$$

where H_b is the wave height at the breaking point, L_o is the deep-water wavelength, and $(h_0)_b$ is the water depth at the breaking point.

The mean water level variation is solved b the time-averaged and depth-integrated momentum equation, given as:

$$\frac{\mathrm{d}S_{xx}}{\mathrm{d}x} = -\rho g(\overline{\eta} + h_0) \frac{\mathrm{d}\overline{\eta}}{\mathrm{d}x}, \tag{13}$$

where S_{xx} is the radiation stress of wave, $\overline{\eta}$ is the mean water level, ρ is the water density, and g is the gravitational acceleration.

A finite-difference scheme with staggered meshes and mid-time grids (Copeland, 1985) was adopted to solve the set of time-dependent mild-slope equations. Two types of geometric boundary conditions are required for computing the boundary value problem: offshore and wall boundaries. Some of the parameters of the rigid porous medium are needed in the computations. The first parameter, inertial coefficient $C_{r,}$ is dependent on the virtual mass effect due to an unsteady flow around a body; it is not readily determined for a randomly and densely packed solid material (Rojanakamthorn *et al*., 1989). Therefore, after Madsen (1974) and Sollitt and Cross (1972), we used $C_r = 1.0$ for the computation. The second parameter is the friction factor, f_b, which can be evaluated based on Lorentz' condition of equivalent work (Sollitt and Cross, 1972). This factor is dependent on the intrinsic permeability, porosity, seepage velocity and the turbulent friction in the porous medium. Their proper values in real applications must be estimated from experiments. For these computations, $f_b = 0.92$ is adopted . The effect of different values of f_b on the wave attenuation on a submerged breakwater will be discussed later on. The third parameter needed for the computations is the porosity of the rigid porous medium, which does not have a wide range of values in the real situation. It was

selected as $\varepsilon_b = 0.4$ after Rojanakamthorn *et al*. (1989).

3. Numerical Results

3.1 Verifications

Fig. 2 shows that the present calculations are valid because they are comparable with the experimental results presented by Rivero *et al*. (1998). It should be noted that the results shown in the figure are for the case without a seawall. These results show that there is a better agreement between the experimental and numerical results if the nonlinear shoaling corrector is considered theoretically. Fig. 2 demonstrates that the modulations of wave height and the mean water level are induced by the reflection in front of the breakwater. In addition, the decay of wave height and the set-up of the water level can be observed clearly as wave passes over the breakwater as the result of the wave breaking. Fig. 3 shows the comparisons of wave height and the mean water level changes between the computed results and experimental data (Chen *et al*., 2007) for the case with a vertical seawall behind the submerged breakwater. This figure also shows a good agreement between the measured and numerical results.

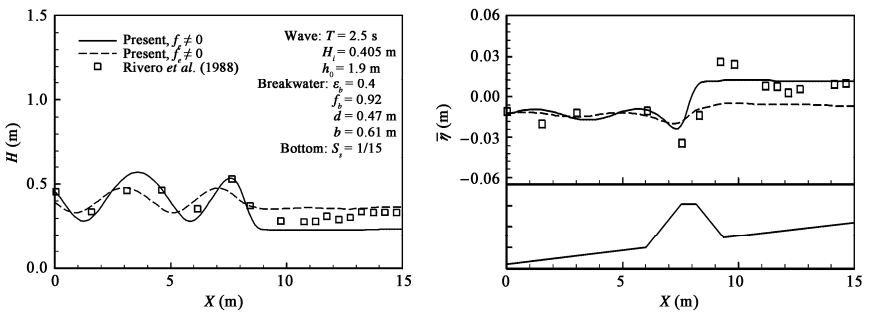

Fig. 2. Comparison of wave height and the mean water level changes between the computed results and experimental data for the case without a seawall.

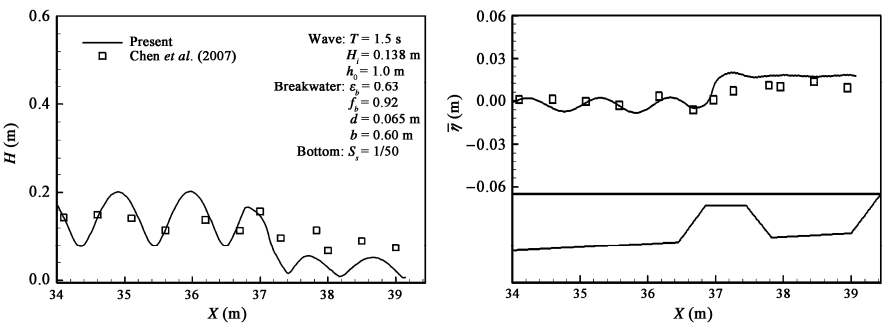

Fig. 3. Comparison of wave height and the mean water level changes between the computed results and experimental data for the case with a seawall.

3.2 Influence of Seawall Types

Two types of seawall, a vertical seawall and an inclined seawall (shown in Figs. 4a and 4b), are

considered in the following numerical simulations for computing wave heights and the mean water levels behind a submerged permeable breakwater. For the case of a vertical seawall, the numerical results of Fig. 5 show the modulation of wave height and nodal points existing between the submerged breakwater and the seawall as the result of the full reflection from the vertical wall. It should be noted that the modulation did not appear behind the submerged breakwater in the case without a seawall as depicted in Fig. 2. The significant modulation of the mean water level can also be observed both in front of and behind the submerged breakwater. This result shows that the wave set-up is significant when $X_s / L_p = 0.25$ and 0.75 (X_s is the distance between the center section of the submerged breakwater and the seawall, and L_p is the wavelength at location X_s); thus, we can find the nodal point of wave height appearing near the top of the submerged breakwater. In addition, higher wave height in front of the submerged breakwater can also be found when $X_s / L_p = 0.25$ and 0.75. In contrast, wave set-down may be found in the cases of $X_s / L_p = 0.50$ and 1.00 so that the wave nodes appear distant from the submerged breakwater.

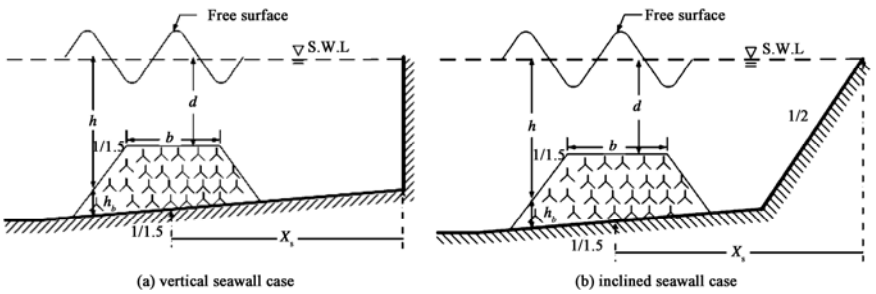

Fig. 4. Definitional sketches of (a) the vertical seawall and (b) the inclined seawall behind the submerged permeable breakwater.

The computed results of different distances between the two structures are shown in Fig. 6 for the case of an inclined seawall behind a submerged breakwater. An obvious wave set-up appears between the submerged breakwater and the inclined seawall when $X_s / L_p = 0.75$, in which the pseudo-node of wave height is near the submerged breakwater. When compared with Fig. 5, the wave height between the submerged breakwater and the inclined seawall is smaller than that of the vertical seawall, due to only the partial reflection from the inclined seawall. In addition, it is clear that the wave set-up increases swiftly at the end of the wall, due to the wave run-up on the inclined seawall.

Fig. 7 shows comparisons of wave height and the mean water level changes among different seawall types when $X_s / L_p = 0.75$. The modulation of wave height and the mean water level variations occur behind the submerged breakwater in the case with a seawall present, but they are generally constant behind the submerged breakwater in the case without a seawall, as described above. Under the same incident wave conditions, larger wave height can be seen in the case of the vertical seawall as the result of the full wave reflection, except near the locations of nodal points. However, the wave set-up behind the breakwater for the cases of both vertical and inclined seawalls is larger than that for the case without a seawall.

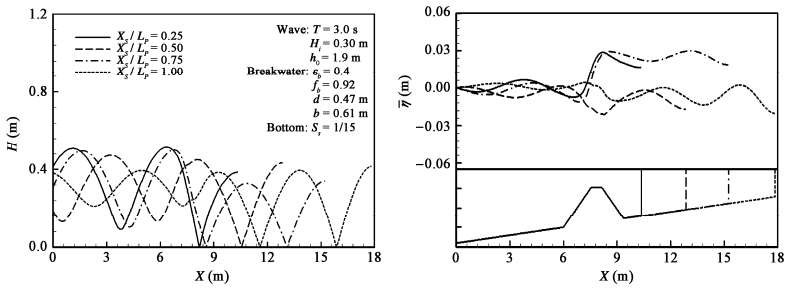

Fig. 5. Wave height and the mean water level changes for different distances between the vertical seawall and the submerged permeable breakwater.

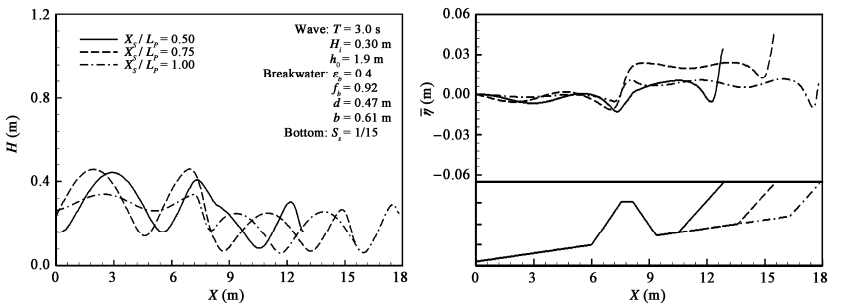

Fig. 6. Wave height and the mean water level changes for different distances between the inclined seawall and the submerged permeable breakwater.

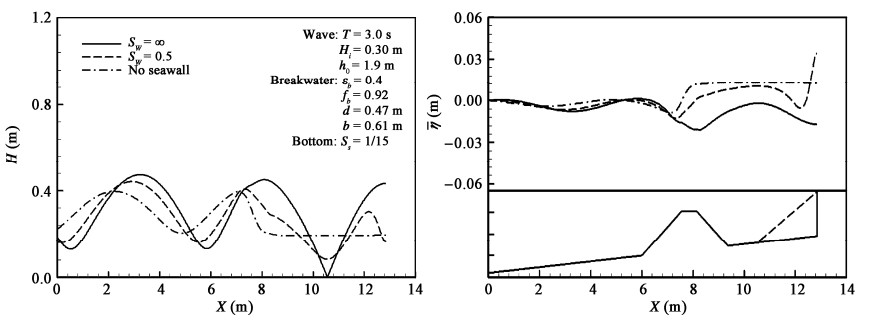

Fig. 7. Comparison of the wave height and the mean water level changes among different seawall types ($X_s / L_p = 0.75$).

3.3 Influence of the Porosity and Friction of the Breakwater

The porosity of the submerged permeable breakwater affects the variations in wave height and water level when $X_s / L_p = 0.75$ for the fixed friction factor $f_b = 0.92$, as shown in Fig. 8. Fig. 8 shows that increasing the porosity of the submerged breakwater produces larger wave height decay and smaller wave set-up behind the submerged breakwater; however, the difference is not significant for different porosities.

In contrast, Fig. 9 shows the influence of the friction factor of the submerged permeable breakwater on variations in wave height and water level when $X_s / L_p = 0.75$ for the fixed porosity $\varepsilon_b = 0.4$. The larger the friction factor of the breakwater is, the higher the water set-up behind the

submerged breakwater will be. However, different friction factors with the fixed porosity do not significantly influence wave height variation behind the breakwater.

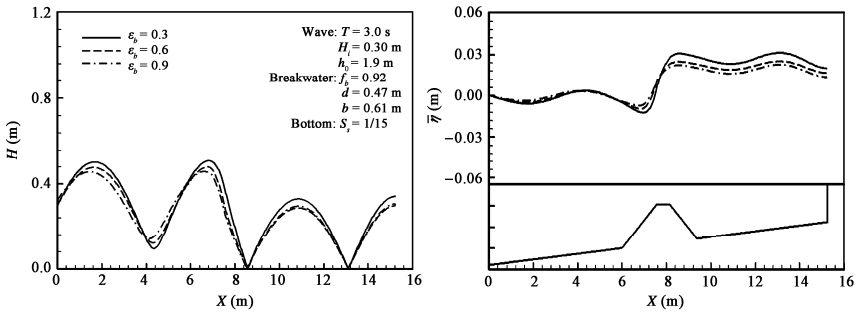

Fig. 8. Wave height and the mean water level evolution for different porosities of the submerged permeable breakwater ($H = 0.3$ m , $X_s / L_p = 0.75$).

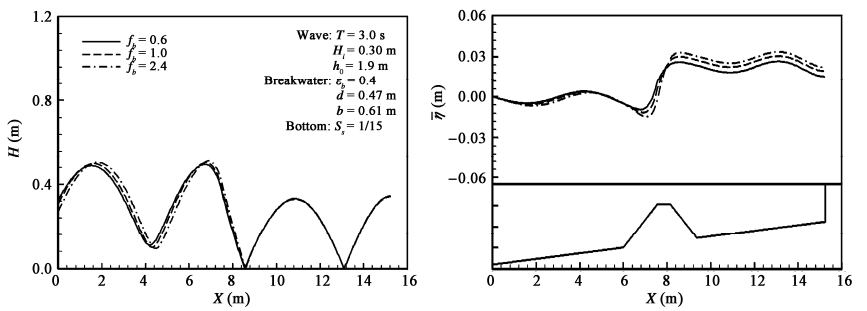

Fig. 9. Wave height and the mean water level evolution for different friction factors of the submerged permeable breakwater ($H = 0.3$ m , $X_s / L_p = 0.75$).

3.4 Influence of Incident Wave Conditions

Fig. 10 shows the wave height and the mean water level changes for different incident wave heights when $X_s / L_p = 0.75$. Furthermore, this figure shows that increasing the incident wave height leads to an increase in the wave set-up between the submerged breakwater and the seawall. In contrast, as shown in Fig. 11, different wave periods will produce different locations of nodal points; the height of the wave set-up is dependent on the locations of nodal points as discussed above regarding Fig. 5.

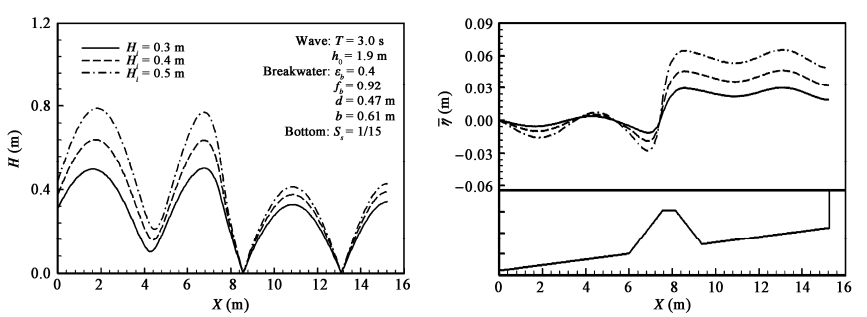

Fig. 10. Wave height and the mean water level evolution for different incident wave heights ($X_s / L_p = 0.75$).

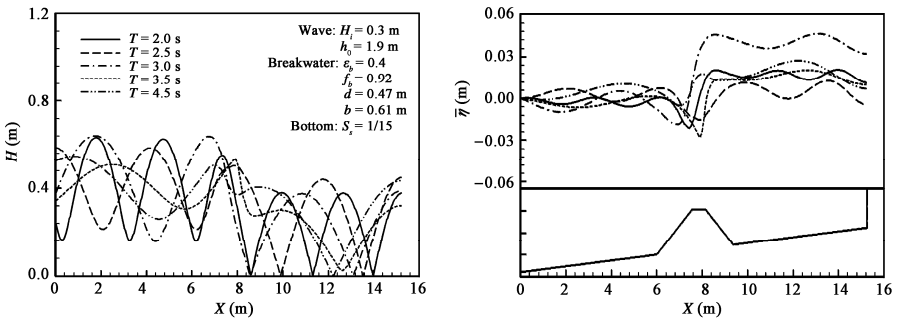

Fig. 11. Wave height and the mean water level evolution for different incident wave periods.

4. Conclusions

We used modified time-dependent mild-slope equations, which involve parameters of the porous medium, to investigate wave height transformation and wave set-up or water piling-up between a submerged permeable breakwater and a seawall. The computed results show that the modulations of the wave profile and wave set-up are clearly observed between the submerged breakwater and the seawall, whereas they stay almost constant for the case without a seawall. A wave node or pseudo-node of wave height evolution could be found between the submerged breakwater and the seawall as a result of the wave reflection from the seawall. We found that the position of the nodal or pseudo-nodal point seems to control the magnitude of the wave set-up. Higher wave set-up can be found if the node or pseudo-node of the wave appears near the top of the submerged breakwater. It is inferred that the nodal point might influence the mass flux from the submerged breakwater to induce the water piling-up; this could be further studied in more detail by use of flow investigations. We also found that the porosity and friction factor of the submerged permeable breakwater could somewhat influence both the wave height transformation and the wave set-up.

References

Chen, H. B., Tsai, C. P. and Chiu, J. R., 2006. Wave reflection from vertical breakwater with porous structure, *Ocean Eng*., **33**(13): 1705~1717.

Chen, H. B., Tsai, C. P. and Jeng, C. C., 2007. Wave transformation between submerged breakwater and seawall, *J. Coast. Res*., SI **50**, 1069~1074.

Copeland, G. J. M., 1985. A practical alternative to the "mild-slope" wave equation, *Coast. Eng*., **9**(2): 125~149.

Dattatri, J., Raman, H. and Jothi Shankar, N., 1978. Performance characteristics of submerged breakwaters, *Proc. 16th Int. Conf. Coast. Eng*., 2153~2171.

Davies, B. L. and Kriebel, D. L., 1992. Model testing of wave transmission past low-crested breakwaters, *Proc. 23rd Int. Conf. Coast. Eng*., 1115~1128.

Diskin, M. H., Vajda, M. L. and Amir, I., 1970. Piling-up behind low and submerged permeable breakwaters, *J. Waterw. Harb. Coast. Eng. Div*., **96**(2): 359~372

Garcia, N., Lara, J. L. and Losada, I. J., 2004. 2-D numerical analysis of near-field flow at low-crested permeable breakwaters, *Coast. Eng*., **51**(10): 991~1020.

Hur, D. S. and Mizutani, N., 2003. Numerical estimation of the wave forces acting on a three-dimensional body on submerged breakwater, *Coast. Eng*., **47**(3): 329~345.

Liu, P. L. F., Lin, P., Chang, K. A. and Sakakiyama, T., 1999. Numerical modeling of wave interaction with porous structures, *J. Waterw. Port Coast. Ocean Eng.*, **125**(6): 322~330.

Losada, I. J., Silva, R. and Losada, M. A., 1996. 3-D non-breaking regular wave interaction with submerged breakwaters, *Coast. Eng.*, **28**(1-4): 229~248.

Loveless, J., Debski, D. and MacLeod, A. B., 1998. Sea level set-up behind detached breakwaters, *Proc. 26th Int. Conf. Coast. Eng.*, 1665~1678.

Madsen, O. S., 1974. Wave transmission through porous structures, *J. Waterw. Harbors Coast. Eng. Div.*, ASCE, **100**(3): 169~188.

Méndez, J. F., Losada, I. J. and Losada, M. A., 2001. Wave-induced mean magnitudes in permeable submerged breakwaters, *J. Waterw. Port Coast. Ocean Eng.*, **127**(1): 7~15.

Rivero, F. J., Arcilla, S. and Gironella, A., 1998. Large-scale hydrodynamic experiments in submerged breakwaters, *Proc. Coast. Dyn.'97*, 754~762.

Rojanakamthorn, S., Isobe, M. and Watanabe, A., 1989. A mathematical model of wave transformation over a submerged breakwater, *Coast. Eng. Japan*, **32**, 209~234.

Rojanakamthorn, S., Isobe, M. and Watanabe, A., 1990. Modeling of wave transformation on submerged breakwater, *Proc. 22nd Int. Conf. Coast. Eng.*, 1060~1073.

Shuto, N., 1974. Nonlinear long waves in a channel of variable section, *Coast. Eng. Japan*, **17**, 1~12.

Sollitt, C. K. and Cross, R. H., 1972. Wave transmission through permeable breakwaters, *Proc. 13th Int. Conf. Coast. Eng.*, 1827~1846.

Tsai, C. P., Chen, H. B. and Hsu, J. R. C., 2001. Calculations of wave transformation across the surf zone, *Ocean Eng.*, **28**(8): 941~955.

Tsai, C. P., Chen, H. B. and Lee, F. C., 2006. Wave transformation over submerged permeable breakwater on porous bottom, *Ocean Eng.*, **33**(11-12): 1623~1643.

Watanabe, A. and Dibajnia, M., 1988. A numerical model of wave deformation in surf zone, *Proc. 21st Int. Conf. Coast. Eng.*, 578~587.